

Atomic Force Microscope Spectroscopy Reveals a Hemifusion Intermediate during Soluble *N*-Ethylmaleimide-Sensitive Factor-Attachment Protein Receptors-Mediated Membrane Fusion

Midhat H. Abdulreda,* Akhil Bhalla,† Edwin R. Chapman,† and Vincent T. Moy*

*University of Miami Miller School of Medicine, Physiology and Biophysics Department, Miami, Florida 33136; and †Howard Hughes Medical Institute and Department of Physiology, University of Wisconsin, Madison, Wisconsin 53706

ABSTRACT This study investigated the effect of soluble *N*-ethylmaleimide-sensitive factor-attachment protein (SNAP) receptors (SNAREs) on the fusion of egg L- α -phosphatidylcholine bilayers using atomic force microscope (AFM) spectroscopy. AFM measurements of the fusion force under compression were acquired to reveal the energy landscape of the fusion process. A single main energy barrier governing the fusion process was identified in the absence and presence of SNAREs in the bilayers. Under compression, a significant downward shift in the fusion dynamic force spectrum was observed when cognate v- and t-SNAREs were present in the opposite bilayers. The presence of vesicle-associated membrane protein (VAMP) and binary syntaxin and SNAP 25 in the apposed bilayers resulted in a reduction in the height of the activation potential by $\sim 1.3 k_B T$ and a >2 -fold increase in the width of the energy barrier. The widening of the energy barrier in the presence SNAREs is interpreted as an increase in the compressibility of the membranes, which translates to a greater ease in the bilayer deformation and subsequently the fusion of the membranes under compression. Facilitation of membrane fusion was observed only when SNAREs were present in both bilayers. Moreover, addition of the soluble cytoplasmic domain of VAMP, which interferes with the interaction between opposing v- and t-SNAREs, prevented such facilitation. These observations implicated the interaction between the cytoplasmic domains of opposing SNAREs in the observed fusion facilitation, possibly by destabilizing the bilayers through pulling on their transmembrane segments. Our AFM compression measurements revealed that SNARE-mediated membrane fusion proceeded through a sequence of two ~ 5 nm collapses of the membrane, an observation that is consistent with the existence of a hemifused state during the fusion process.

INTRODUCTION

Soluble *N*-ethylmaleimide-sensitive factor-attachment protein (SNAP) receptors (SNAREs) are recognized as fusion proteins and have been widely accepted as the minimal machinery for membrane fusion (1). SNAREs associated with the vesicular membrane are termed v-SNAREs, and those associated with the target plasma membrane are t-SNAREs. The neuronal v-SNARE, vesicle-associated membrane protein 2 (VAMP 2, also referred to as synaptobrevin 2) and the t-SNAREs, syntaxin and synaptosomal-associated protein 25 kD (SNAP 25) are expressed in the presynaptic terminal and mediate membrane fusion during neurotransmitter release (2,3). The interaction between the v- and t-SNAREs forms a ternary core complex that has been described as a parallel α -helical bundle or a coiled coil structure (4,5). It is well established that VAMP and syntaxin contribute one helix each, whereas SNAP 25 contributes two helices to the complex. VAMP and syntaxin are anchored via their transmembrane segments in the vesicular and plasma membranes, respectively, whereas SNAP 25 is recruited via palmitoylation sites to the plasma

membrane, where it interacts with syntaxin. The SNARE hypothesis proposes that the interaction between v- and t-SNAREs mediates vesicle fusion with the plasma membrane (6–8). After arrival of an action potential to the presynaptic terminal, increasing intracellular Ca^{2+} is sensed by the putative Ca^{2+} sensor in the vesicle surface, synaptotagmin. It is speculated that upon sensing of Ca^{2+} , synaptotagmin interacts with phospholipids and the SNAREs leading to the full zippering of the SNARE complex, which ultimately leads to the formation of the fusion pore and neurotransmitter release (9).

There are currently two main models for fusion pore formation: the proximity model and the protein-lined fusion pore model (10). The proximity model proposes a mechanical role for the SNARE proteins while zippering, which brings the apposed bilayers into a critical proximity where nucleation of a purely lipidic fusion pore can take place and membrane fusion can ensue. During this process, the two membranes merge together, passing through a hemifused state (11,12). Hemifusion involves the coalescence of the two proximal leaflets (monolayers) followed by that of the remaining distal monolayers of the apposed membranes when full fusion is complete (13). Given the high energy cost for the initiation and opening of the fusion pore (14), the proximity model falls short in explaining the reversible kiss-and-run fusion events observed in vivo (15–19) and, thus, the protein-lined fusion pore model has been invoked

Submitted June 4, 2007, and accepted for publication September 5, 2007.

Address reprint requests to Vincent T. Moy, University of Miami Miller School of Medicine, Physiology and Biophysics Department, 1600 NW 10th Ave., Miami, FL 33136. Tel.: 305-243-3201; Fax: 305-243-5931; E-mail: vmoy@miami.edu.

Editor: David D. Thomas.

© 2008 by the Biophysical Society
0006-3495/08/01/648/08 \$2.00

doi: 10.1529/biophysj.107.114298

(20–22). In this model, a gap junction type of structure for the fusion pore is proposed (23). During formation of the SNARE complex, the SNAREs pull together and their transmembrane segments begin to oligomerize (24–26) in the apposed membranes to form hemichannel-like structures (20,27). Upon formation of these structures, an open channel (i.e., fusion pore) forms whereby vesicular content is released into the extracellular space (28,29). A fusion pore behaving like an ion channel can account for the fast opening and closing during the reversible kiss-and-run fusion events. Moreover, the protein-lined pore is a transient structure and, upon dilation, the transmembrane segments dissociate and lipid molecules are incorporated into the pore as full membrane fusion takes place.

Different approaches have been employed to investigate the role of SNAREs in membrane fusion (7,11,25,30,31). Although, SNAREs have been widely shown to be sufficient in driving membrane fusion, recent studies have challenged the requirement for SNAP 25 in the SNARE complex during vesicle fusion with planar membranes (32,33). Nonetheless, the specific mechanism for SNARE-mediated membrane fusion is yet to be established. We previously reported on a protein-free lipid bilayer system which provided the necessary spatial and temporal resolution to detect fusion events and measure fusion forces using atomic force microscopy (AFM) (34). In this study, we use this system to measure forces required to generate fusion of apposed egg L- α -phosphatidylcholine (egg PC) bilayers containing SNARE proteins in an effort to investigate the mechanism(s) of SNARE-mediated membrane fusion.

MATERIALS AND METHODS

Atomic force microscope

We used a custom-built AFM in which the lateral and vertical scans are decoupled (35). In brief, the sample sits on an X-Y stage which can be adjusted relative to the cantilever mounted on a stacked piezoelectric transducer (Physik Instrumente, Auburn, MA). The piezoelectric transducer provides the necessary vertical movement (0– \sim 10 μ m range) to approach and retract the cantilever from the stationary substrate. AFM cantilevers were purchased from Veeco (model MLCT-AUHW, part 00-103-0925; Woodbury, NY), and the largest V-shaped cantilever with a nominal spring constant of 10 mN/m was used in all experiments after attachment of a glass microbead (\sim 50 μ m diameter; Polysciences, Warrington, WA). Custom software was used to calibrate the cantilever tip based on thermal noise analysis (36) and to control the position of the piezoelectric transducer and timing during force scan measurements. A charge-coupled device camera was used to visualize the sample through a 20 \times objective positioned beneath the stage. To maintain desired sample temperature, a Peltier element was positioned underneath the sample chamber and a silicone-based heat sink compound was used to provide thermal coupling with the sample chamber. A temperature probe was positioned in direct contact with the buffer bathing the sample, and temperature stability was within 0.3°C.

Glass dish and cantilever preparation

Glass microbeads were epoxied to the tip of the silicone nitride cantilevers with the aid of a micromanipulator. Glass dishes and stainless steel utensils

were boiled in distilled water containing \sim 10% RBS 35 detergent (Pierce, Rockford, IL) and ethanol and rinsed extensively with distilled water. Cantilevers with attached microbeads were soaked in 1% *n*-octyl β -D-glucopyranoside, then in 100% ethanol followed by ultraviolet irradiation after extensive rinsing in nanopure water (18 M Ω cm; Barnstead, Dubuque, IA). Finally and immediately before use, cleaned cantilevers and glass dishes were further treated for 5 min in a nitrogen plasma cleaner (Harrick Plasma, Ithaca, NY). The hydrophilic nature of the surfaces was confirmed by the presence of electrostatic repulsion between the glass substrates and ionic screening when AFM force scans were performed in purified water and salt solutions, respectively (data not shown).

AFM measurement of fusion force

During an AFM force scan measurement, the approach and retract traces correspond to the movement of the cantilever tip toward and away from the substrate, respectively. As the cantilever is lowered and pressed against the substrate, the cantilever is subjected to forces that result in its bending (deflection). Deflection of the cantilever is monitored by the position of a pigtail laser beam focused on the coated back side of the cantilever tip and reflected onto a two-segment photodiode. Upward or downward cantilever deflections signify, respectively, repulsive or attractive interaction forces between the cantilever tip and the sample. The change of the laser position on the photodiode is calibrated based on the force causing the cantilever deflection. All force measurements are performed in Tris-buffered saline (TBS) (10 mM Tris/100 mM NaCl, pH 7.2). The interaction force between the cantilever and the substrate is derived from the product of the spring constant of the cantilever and the extent of its deflection. The resulting force scan represents the interaction force versus displacement of the piezoelectric transducer. Since fusion of the compressed bilayers occurs during the approach step, in this study, we focused on the approach trace of the AFM force scan.

Custom data analysis programs were written in *Igor* software to detect the jump events during the approach step of the force scans. These jump events were interpreted as signatures for hemifusion and fusion of the bilayers. The forces associated with the jump events were also measured. We only reported forces measured at the first jump event. We typically carried out 300–400 force scan measurements for each compression rate, and a range over \sim 2 orders of magnitude of compression rates was covered by varying the scan velocity. A minimum of triplicate experiments for each condition was performed on different days. From 20 to 30% of the force scans produced jump events, and the measured forces were grouped in histograms (10 pN bin size). The most probable force for each compression rate was derived, and plots of force versus compression rate were generated. These plots are also referred to as the dynamic force spectrum (DFS).

Plasmids and protein purification

Plasmids to generate recombinant full length VAMP 2 (pTW2) and the full length t-SNARE heterodimer (syntaxin 1A and SNAP 25; pTW34) (1) were provided by J. E. Rothman (Columbia University, New York, NY). Complementary DNA encoding full length syntaxin 1A (37) (provided by R. H. Scheller; Genentech, San Francisco, CA) was subcloned into a pTrc-His vector (Invitrogen Life Technologies, Carlsbad, CA), resulting in an N-terminal His-6 tag. Proteins were expressed and purified as described (30,38). Briefly, bacterial pellets were resuspended in 25 mM HEPES-KOH, 400 mM KCl, 20 mM imidazole, and 5 mM β -mercaptoethanol. Bacterial extracts were mixed with nickel-nitrilotriacetic acid agarose (Qiagen, Valencia, CA) for 2 h at 4°C. Beads were washed two times in wash buffer (25 mM HEPES-KOH, 400 mM KCl, 20 mM imidazole, and 5 mM β -mercaptoethanol, 1 mM MgCl₂) plus 10 μ g/ml DNase and RNase (Roche Applied Science, Indianapolis, IN) to remove residual RNA/DNA. Two more washes were carried out in the resuspension buffer. Proteins were eluted from the beads in resuspension buffer with 500 mM imidazole, 10% glycerol (w/v), and 1% *n*-octylglucoside (Research Products International,

Philadelphia, PA). SNAP 25 and the soluble cytoplasmic domain of VAMP (cd-VAMP; residues 1–94; pET-rsybCD, also provided by J. E. Rothman) were purified as above except that *n*-octylglucoside was omitted from the elution buffer, and soluble protein was dialyzed using dialysis tubing from Spectrum Labs (Rancho Dominguez, CA) against 25 mM HEPES-KOH, 100 mM KCl, 10% glycerol (w/v), and 1 mM dithiothreitol.

Reconstitution of SNAREs into vesicles and bilayer formation

Egg PC was purchased from Avanti Polar Lipids (Alabaster, AL). Reconstitution of v-SNARE and t-SNARE vesicles was carried out as previously described (30,38) with modifications. In brief, v-SNARE and binary t-SNAREs were reconstituted in separate populations of 100% egg PC vesicles by the detergent depletion method followed by a floatation step on an Accudenz density gradient, as previously described (38). Protein concentrations were adjusted to yield an average of 25 copies of protein molecules per vesicle. SNARE-free vesicles were prepared as described previously (30) but using 100% egg PC. For each experiment, the bilayers were formed by vesicle adsorption and fusion to the hydrophilic surfaces. Egg PC vesicles, with and without SNAREs, were adsorbed for 1 h at 4°C, separately, to cleaned glass dishes and the glass microbeads attached to the cantilever tip. After adsorption and while always in solution, the bilayers were gently washed three times with TBS. The AFM was assembled next, and necessary temperature adjustments were performed before initiation of the experiments.

RESULTS

SNARE-mediated membrane fusion

VAMP 2 (v-SNARE) and binary syntaxin 1A and SNAP 25 (t-SNAREs) were reconstituted into egg PC bilayers. AFM fusion force measurements were carried out at ~24°C in the absence and presence of these cognate v- and t-SNAREs in the opposite bilayers. Separately, the v-SNARE bilayers were formed on the glass microbead attached to the cantilever tip, and the t-SNARE bilayers were formed on the glass dish. The AFM was later assembled with the bilayers being always submerged in TBS. As previously described (34), during a force scan measurement, the apposed bilayers are compressed together during the approach step, which leads to an upward deflection of the cantilever (Fig. 1). With the applied compression, the bilayers hemifuse (J_1) and eventually fully fuse (J_2) with the continued application of compression. The jump is attributed to the sudden displacement of the cantilever tip toward the substrate as a result of the coalescence of the lipid material at the interface between the substrates bearing the bilayers. The fusion force is measured at the beginning of the jump event, and only fusion forces associated with the first jump (J_1) are reported. The measured forces were grouped in distribution histograms based on the compression rate (Fig. 2 A). Different compression rates were achieved by varying the scan velocity. As evident in Fig. 2 A, the fusion force was reduced in the presence of SNAREs in the bilayers. The most probable force was obtained from the histograms and plotted against the logarithm of the compression rate, also referred to as the DFS (Fig. 2 B). The DFS revealed that the fusion force increased linearly with the logarithm of the compression rate.

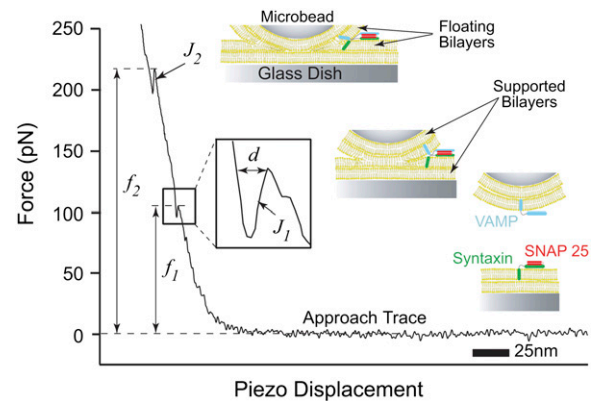


FIGURE 1 Typical force versus piezo displacement curve displaying the approach trace of an AFM force scan measurement between apposed floating lipid bilayers containing SNAREs. As the bilayers are compressed together, they fuse in two jump steps at J_1 and J_2 . The jump is due to the sudden displacement of the cantilever tip toward the substrate as a result of the merger of the bilayers under the applied compression force f_1 or f_2 . The inset is a magnification of the approach trace during the jump event. Distance d is the measure of the jump distance and is consistently on the order of a single egg PC bilayer thickness. This suggests the merging of the two proximal monolayers (hemifusion) of the apposed bilayers during J_1 followed by that of the two distal ones (full fusion) during J_2 as depicted in the accompanying cartoons.

A significant reduction in the fusion force over the entire range of the compression rate was observed when SNARE proteins are present in the bilayers as opposed to when they are absent (Fig. 2 B). Moreover, the absence of VAMP from the v-SNARE bilayers, or the addition of 20 μ M of the soluble cytoplasmic domain of VAMP (cd-VAMP), interfered with the observed reduction in the compression force that is required to generate fusion of the apposed membranes (Fig. 2 B). These data indicate that *trans*-SNARE pairing is required during SNARE-mediated membrane fusion in this assay system.

Hemifusion during SNARE-mediated membrane fusion

At a protein/lipid ratio of 1:1000 used to form our bilayers, we estimate an average protein density of 0.17 ± 0.04 molecule per μm^2 . With this surface density we noticed that a majority, but not all, of the AFM measurements revealed signatures of SNARE-mediated fusion where simultaneous jump and unbinding events are detected in the approach and retract steps, respectively. As noted earlier, membrane fusion is characterized by two jumps in the AFM approach trace (Fig. 1), one corresponding to hemifusion and a second, at higher force, to full fusion. In general, SNARE-mediated hemifusion requires lower compression forces (see Figs. 2 and 5 A, left panel). In addition, we noted that SNARE-mediated hemifusion is associated with adhesion of the membranes detected in the retraction trace of the AFM force scan measurement (see Fig. 5 A, left panel). The measured adhesive forces, in the range of 50–300 pN, are consistent with the unbinding forces

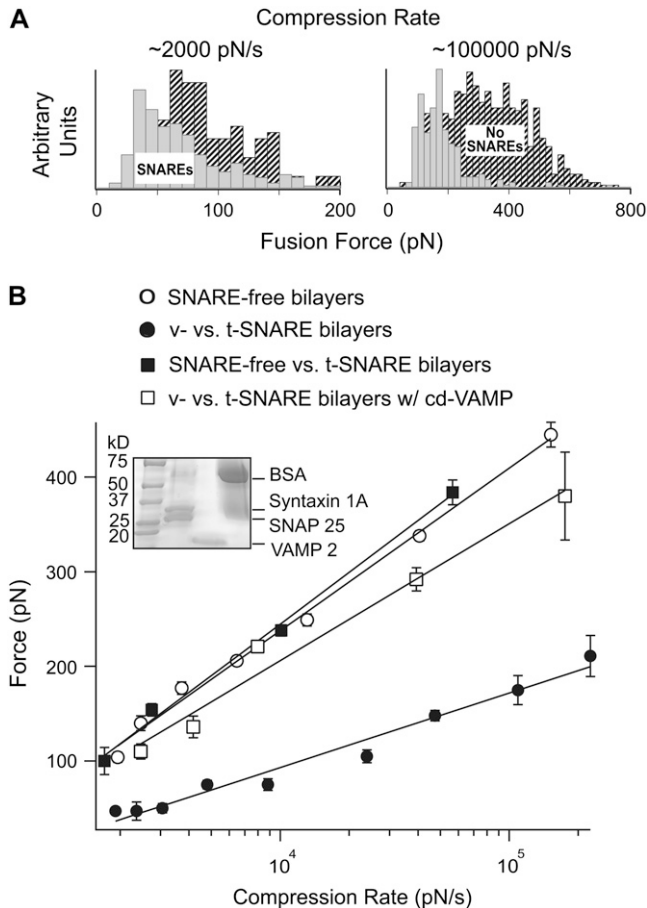


FIGURE 2 (A) Distribution histograms of fusion force values measured at the first jump during the approach step of an AFM force measurement. The forces measurements were carried out under different compression rates (~ 2000 and $\sim 100,000$ pN/s) in the absence (*shaded*) and presence (*hatched*) of SNAREs in the bilayers. (B) Dynamic force spectra of the fusion process for egg PC bilayers with and without SNAREs. Notice the significant decrease in the fusion force when cognate v-SNARE (VAMP 2) and t-SNAREs (binary syntaxin 1A and SNAP 25) were present in the bilayers as compared to SNARE-free bilayers. The inset shows sodium dodecylsulfate-polyacrylamide gel electrophoresis confirming the successful reconstitution of VAMP or syntaxin and SNAP 25 in v- and t-SNARE vesicles, respectively. No change in the force profile was observed when v-SNARE bilayers were substituted with SNARE-free bilayers. Similarly, treatment of the t-SNARE bilayers with the soluble cytoplasmic domain of VAMP (cd-VAMP, $20 \mu\text{M}$) prevented reduction in the fusion force that was observed for intact v- and t-SNARE bilayers. Lines are fits of the model to the data points. Error bars are the standard error of the mean.

of individual SNARE complexes (M. H. Abdulreda and V. T. Moy, unpublished observations) (39,40). In contrast, compression of SNARE-free bilayers did not show evidence of adhesion in the retraction trace (see Fig. 5 A, right panel). Using the adhesion event as a signature for SNARE-mediated fusion, we estimate that $\sim 65\%$ of our fusion measurements were facilitated by SNAREs. Our analysis revealed that in SNARE-mediated fusion, the jump distance for hemifusion was reduced from 4.4 ± 0.1 nm to 3.9 ± 0.3 nm (see Fig. 5 B).

As discussed below, this reduction in jump distance can be attributed to the greater compressibility of SNARE-containing bilayers. Moreover, our AFM measurements lend support to a model in which SNARE-mediated membrane fusion proceeds through hemifusion.

DISCUSSION AND CONCLUSIONS

Using the AFM, we carried out dynamic force measurements to reveal the energy landscape of the fusion process for egg PC bilayers. Our results showed that, under compression, the fusion force was significantly reduced when SNARE proteins were present in the bilayers. More specifically, the fusion force was most reduced when cognate v- and t-SNAREs were present in the opposite bilayers. Using a previously described model (34), we can elaborate on the role of SNARE proteins in the fusion process. In brief, the model is based on the transition state theory, where an energy barrier has to be overcome for fusion to occur. The unfused bilayers pass through a transition state that is at the peak of the energy barrier as they move along the reaction coordinate toward the fused state. Under the application of a compression force, the applied force adds a linear term to the thermopotential of the system, which effectively tilts the barrier and reduces the activation potential of the process. The fusion rate under compression (f) can then be expressed as

$$k_{\text{fusion}} = k^{\circ} \exp \left\{ \frac{f\gamma}{k_{\text{B}}T} \right\}, \quad (1)$$

where k° is the fusion rate in the absence of applied compression and describes the energy barrier height, γ is the distance between the unfused and the transition state positions along the reaction coordinate and describes the energy barrier width, k_{B} is the Boltzmann constant, and T is the absolute temperature.

Equation 1 describes how the fusion rate is changed by constant compression forces. However, a constant compression force is difficult to maintain in an AFM experiment. Instead, a dynamic force approach was used to characterize the forces leading to fusion of the compressed bilayers. Under conditions of constant compression rate r_f ($r_f = df/dt$), the probability density function for forced fusion is given by

$$P(f) = k^{\circ} \exp \left\{ \frac{\gamma f}{k_{\text{B}}T} \right\} \exp \left\{ \frac{k^{\circ} k_{\text{B}}T}{\gamma r_f} \left[1 - \exp \left(\frac{\gamma f}{k_{\text{B}}T} \right) \right] \right\}, \quad (2)$$

and the most probable force f^* (i.e., the maximum of the distribution $\partial P(f)/\partial f = 0$) can be expressed as

$$f^* = \frac{k_{\text{B}}T}{\gamma} \ln \left\{ \frac{\gamma}{k^{\circ} k_{\text{B}}T} \right\} + \frac{k_{\text{B}}T}{\gamma} \ln \{r_f\}. \quad (3)$$

Equation 3 shows that the most probable fusion force f^* is a linear function of the natural logarithm of the compression or loading rate $\ln\{r_f\}$. The fusion parameters k° and γ (Table 1) were derived from fitting Eq. 3 to the acquired plots of f^* versus $\ln\{r_f\}$ (DFS). Using these parameters, we can estimate

TABLE 1 Energy barrier parameters of the fusion process for egg PC bilayers in the absence or presence of SNAREs in the specified combinations

Bilayers	Energy barrier parameters	
	γ (Å)	k° (s ⁻¹)
SNARE-free versus SNARE-free	0.5	5.52
v- versus t-SNAREs	1.2	19.3
SNARE-free versus t-SNAREs	0.52	5.67
v- versus t-SNAREs w/cd-VAMP	0.65	6

Fusion was generated by compressing the bilayers that were present on the opposite hydrophilic substrates, the glass dish, and microbead attached to the AFM tip. The parameters were derived using the above model. Notice the >2-fold increase in the barrier width and ~4-fold increase in the fusion rate when v- and t-SNARE proteins existed in the bilayers. See Fig. 3 for an interpretation of these parameters in terms of the energetics of the fusion reaction.

the relative position of the transition state along the fusion energy landscape between two similar systems, where relative differences in the height and width of the energy barrier between the systems under different conditions can be compared.

Fig. 3 shows that during the fusion process, the bilayers pass along the reaction coordinate from the unfused to the fused state passing through a transition state, which is at the peak of the energy barrier. The distance between the positions of the unfused and the transition state is the energy barrier width (γ). k° describes the height of the energy barrier or the activation potential of the membrane fusion process.

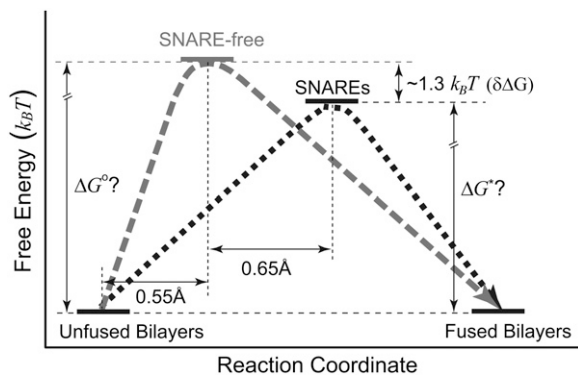


FIGURE 3 Energy landscape of the fusion process in the absence of compression was revealed by our AFM experiments. Based on the transition state theory, the unfused bilayers move along the reaction coordinate toward the fused state, passing through a transition state that is at the peak of the energy barrier. In the presence of cognate v- and t-SNAREs in the apposed bilayers, the energy barrier width was increased and the position of the transition state was shifted to the right by 0.65 Å relative to the SNARE-free bilayers. The height of the energy barrier was also reduced by $\sim 1.3 k_B T$. Both changes lead to a reduction in the slope of the energy barrier. A steeper barrier is harder to overcome. Thus, the reduction in the slope of the barrier, effectively, results in a facilitation of the overall process. We interpret the widening in the energy barrier as an increase in the minimal separation distance between the apposed bilayers before fusion can take place. Figure not to scale.

The derived energy barrier parameters (Table 1) showed that the energy barrier width was increased by >2-fold and its height was reduced by $\sim 1.3 k_B T$ ($\delta\Delta G$) in the presence of cognate v- and t-SNAREs in the bilayers as compared to SNARE-free bilayers. The relative difference in the energy barrier height $\delta\Delta G$ between two systems is given by

$$\delta\Delta G = -k_B T \ln \left(\frac{k_1^\circ}{k_2^\circ} \right), \quad (4)$$

where, k_1° and k_2° are the fusion rate constants of the compared systems 1 and 2, respectively. More specifically, in the presence of SNAREs in the bilayers, the position of the transition state was shifted along the reaction coordinate to the right due to widening of the energy barrier (1.2 Å), and its position along the free energy axis (height) was lowered. The overall effect of these modifications is a reduction in the slope of the energy barrier, which effectively results in a facilitation of the fusion process. Similar to our previous observation upon addition of cholesterol (34), the presence of SNAREs in the bilayers had more prominent effects on the width of the energy barrier than its height. In the presence of SNAREs in the bilayers, widening of the energy barrier, in the absence of compression, is interpreted as an increase in the compressibility of the bilayers, which translates to a greater ease in the deformation of the membranes and subsequently their fusion under compression. This is illustrated in Fig. 3 where interpretation of our results, in terms of the above model, shows that the interaction between SNARE proteins in the opposite bilayers facilitated membrane fusion in the absence of compression. However, such facilitation becomes more apparent during accelerated fusion under compression (Fig. 4). It is evident in Fig. 4 that, in the presence of SNAREs, the fusion rate is initially ~4-fold

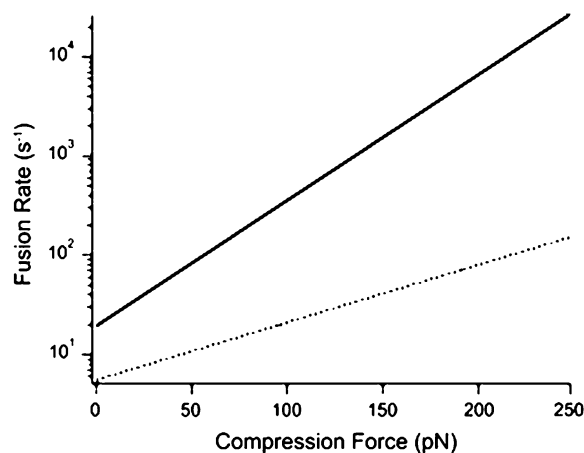


FIGURE 4 Fusion rate increases when SNARE proteins are present in the bilayers, with and without compression. However, according to Eq. 1, the rate increases exponentially with applied compression force. Using Eq. 1, rate values were derived in the absence (dotted line) and presence (solid line) of cognate v- and t-SNAREs in the opposite bilayers. The derived values were plotted against the corresponding compression force.

higher than that in their absence, and the difference between the rates increases exponentially with compression force.

During neurotransmitter release, continuity between the lumen of the vesicle and the extracellular space is provided through the opening of a fusion pore. According to the protein-lined pore model, mixing of the proximal monolayers (hemifusion) may or may not occur on the way toward full membrane fusion. Furthermore, whether or not membrane fusion proceeds through hemifusion, there will be no change in the distance spanning the two membranes until both bilayers have fully merged and permanent fusion has taken place. At this point, the distance is reduced by an amount equivalent to two bilayer thicknesses. This is in sharp contrast to the proximity model where the distance changes in two discernable steps, each equivalent to one bilayer thickness—the first after hemifusion and the second as a result of full fusion. In our AFM system, we are able to measure the jump distance during hemifusion (d ; inset in Fig. 1), and we consistently measure a jump distance of 3.9 ± 0.3 nm in the presence of SNARE proteins in the bilayers (Fig. 5 B). Due to the fact that we detect a jump and the jump distance is consistently on the order of a single bilayer thickness, our findings are consistent with a model where bilayers transition through a hemifused state during membrane fusion.

Our experiments were designed to determine the minimal number of SNARE complexes required to mediate membrane fusion. To achieve these conditions, we used a low surface density (0.17 ± 0.04 molecule per μm^2) of SNAREs in the bilayers. Subsequently, 20–30% of the force scans yielded jump events, and $\sim 65\%$ of those scans showed unbinding events corresponding to the interaction between SNARE proteins (Fig. 5 A, left panel). Additional analysis of these unbinding events indicated that they resulted from the unbinding of single SNARE complexes (39,40). This analysis revealed that the observed fusion facilitation was yielded by single interactions between SNARE proteins. Given the nature of our experimental system, bilayer fusion is ensured by the applied compression; and although other studies have suggested that a single SNARE complex is sufficient to dock and fuse a vesicle to a planar lipid bilayer (32,40), we cannot currently confirm whether the observed fusion facilitation mediated by a single SNARE complex is sufficient to produce membrane fusion *in vivo*. Nevertheless, our results indicate that the formation of a protein-lined pore, involving multiple SNARE complexes, is not required for bilayer fusion in our experimental system.

The proximity model for membrane fusion does not implicate the direct involvement of SNARE proteins in the formation of a fusion pore. It suggests that SNAREs contribute to the work performed on the bilayers during membrane fusion (41,42); the interaction between SNARE proteins brings the membranes to a minimal distance, a critical proximity, where membranes undergo spontaneous lipid mixing and, ultimately, fusion. In our experiments, however, the AFM provides the necessary mechanical force to induce

fusion, with and without SNAREs. If SNARE interactions were to facilitate fusion by only contributing to the mechanical work, their contribution would be overwhelmed by the higher AFM-applied compression, and we would have expected to see no change in the fusion force under compression. Yet, the fusion force was reduced when SNAREs existed in both bilayers but not in a single bilayer or when opposing SNARE interactions were prevented by soluble cd-VAMP (Fig. 2 B). This suggested an additional role for SNARE interaction in destabilizing the membranes during SNARE-mediated fusion. Such a role could be brought about by pulling on the SNARE transmembrane segments as “tension” is generated during zippering of the *trans*-SNARE complex. It has been shown that replacing the transmembrane segment of either v- or t-SNAREs with a lipid anchor prevents fusion between vesicles (43). Moreover, increasing

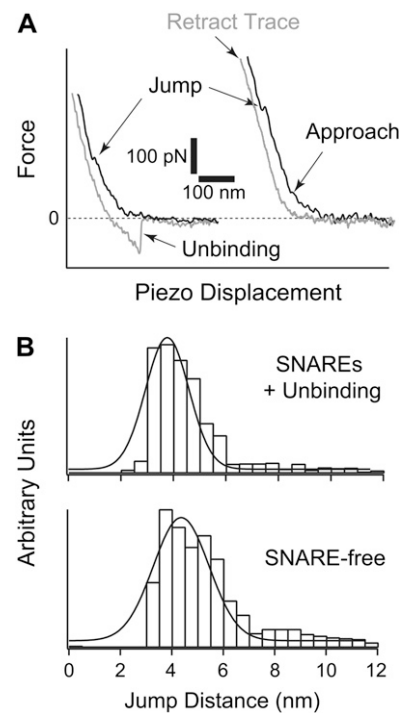


FIGURE 5 (A) Representative approach and retract traces from AFM force measurement. In the presence of SNAREs in the bilayers (left panel), hemifusion (jump) was observed during approach at a lower compression force, and unbinding events were detected in the retract step. These unbinding events indicated SNARE-mediated fusion. On the other hand, higher compression forces were measured for hemifusion and no unbinding events were detected during the retract step in the absence of SNAREs (right panel). (B) Distribution histograms for jump distance values (d ; inset in Fig. 1) measured during jump events in the presence (top) or absence (bottom) of SNAREs in the bilayers. The top panel shows jump distance values that were measured in the presence of simultaneous unbinding events in the retract step. A shift in the jump distance value was observed when SNAREs existed in the bilayers. It was reduced from 4.4 ± 0.1 nm to 3.9 ± 0.3 nm, which is interpreted as an increase in the compressibility and deformation of the membranes when SNAREs are present in the bilayers. The increase in the compressibility and deformation of the membrane translates into a greater ease in membrane fusion.

the length of a flexible linker between the cytoplasmic and transmembrane segments reduced the fusion efficiency in a linker length-dependent manner (42). Therefore, we speculate that pulling on the transmembrane segments leads to their tilting or upward movement in the membrane in which they are anchored, which in turn destabilizes the lipid bilayers at the interface between the apposed membranes. This promotes the nucleation of a fusion pore and may lead to fusion.

In conclusion, our results show that SNARE-mediated bilayer fusion proceeds through hemifusion. They also suggest that as few as one SNARE complex is sufficient to significantly reduce the energy requirements for the fusion process under compression and possibly mediate membrane fusion. In the presence of SNAREs, the fusion rate of the bilayers increases exponentially during accelerated fusion under compression. It also increases in the absence of applied compression. This increase in the fusion rate is the result of the overall reduction in the slope of the energy barrier and is interpreted as an increase in the compressibility of the membranes, which translates to a greater ease in the deformation of the membranes and subsequently their fusion. These findings lend support to a model for SNARE-mediated membrane fusion where interaction between *trans*-SNAREs lead to local destabilization of the lipid bilayers and subsequently to hemifusion on the path to full fusion.

We thank C. Freites for custom fabrications and B. Yuan, M. Höefling, and C. Chu for help with software development. We also thank Dr. Y. Qin for help with Western blots and Dr. F. Rico for insightful feedback. We thank Drs. J. E. Rothman and R. H. Scheller for the protein constructs. Dr. E. R. Chapman is an investigator of the Howard Hughes Medical Institute.

This work was supported by the National Institutes of Health (grants GM55611 (M.H.A. and V.T.M.), GM56827 (A.B. and E.R.C.), and MH61876 (A.B. and E.R.C.)) and the American Heart Association (0440168N (A.B. and E.R.C.)).

REFERENCES

- Weber, T., B. V. Zemelman, J. A. McNew, B. Westermann, M. Gmachl, F. Parlati, T. H. Sollner, and J. E. Rothman. 1998. SNAREpins: minimal machinery for membrane fusion. *Cell*. 92:759–772.
- Chen, Y. A., and R. H. Scheller. 2001. SNARE-mediated membrane fusion. *Nat. Rev. Mol. Cell Biol.* 2:98–106.
- Jahn, R., and T. C. Sudhof. 1999. Membrane fusion and exocytosis. *Annu. Rev. Biochem.* 68:863–911.
- Poirier, M. A., W. Xiao, J. C. Macosko, C. Chan, Y. K. Shin, and M. K. Bennett. 1998. The synaptic SNARE complex is a parallel four-stranded helical bundle. *Nat. Struct. Biol.* 5:765–769.
- Sutton, R. B., D. Fasshauer, R. Jahn, and A. T. Brunger. 1998. Crystal structure of a SNARE complex involved in synaptic exocytosis at 2.4 Å resolution. *Nature*. 395:347–353.
- Sollner, T., S. W. Whiteheart, M. Brunner, H. Erdjument-Bromage, S. Geromanos, P. Tempst, and J. E. Rothman. 1993. SNAP receptors implicated in vesicle targeting and fusion. *Nature*. 362:318–324.
- Nickel, W., T. Weber, J. A. McNew, F. Parlati, T. H. Sollner, and J. E. Rothman. 1999. Content mixing and membrane integrity during membrane fusion driven by pairing of isolated v-SNAREs and t-SNAREs. *Proc. Natl. Acad. Sci. USA*. 96:12571–12576.
- Brunger, A. T. 2005. Structure and function of SNARE and SNARE-interacting proteins. *Q. Rev. Biophys.* 38:1–47.
- Chapman, E. R. 2002. Synaptotagmin: a Ca(2+) sensor that triggers exocytosis? *Nat. Rev. Mol. Cell Biol.* 3:498–508.
- Jackson, M. B., and E. R. Chapman. 2006. Fusion pores and fusion machines in Ca(2+)-triggered exocytosis. *Annu. Rev. Biophys. Biomol. Struct.* 35:135–160.
- Yoon, T. Y., B. Okumus, F. Zhang, Y. K. Shin, and T. Ha. 2006. Multiple intermediates in SNARE-induced membrane fusion. *Proc. Natl. Acad. Sci. USA*. 103:19731–19736.
- Lu, X., F. Zhang, J. A. McNew, and Y. K. Shin. 2005. Membrane fusion induced by neuronal SNAREs transits through hemifusion. *J. Biol. Chem.* 280:30538–30541.
- Jahn, R., T. Lang, and T. C. Sudhof. 2003. Membrane fusion. *Cell*. 112:519–533.
- Reese, C., and A. Mayer. 2005. Transition from hemifusion to pore opening is rate limiting for vacuole membrane fusion. *J. Cell Biol.* 171:981–990.
- Wang, C. T., J. Bai, P. Y. Chang, E. R. Chapman, and M. B. Jackson. 2006. Synaptotagmin-Ca2+ triggers two sequential steps in regulated exocytosis in rat PC12 cells: fusion pore opening and fusion pore dilation. *J. Physiol.* 570:295–307.
- Harata, N. C., S. Choi, J. L. Pyle, A. M. Aravanis, and R. W. Tsien. 2006. Frequency-dependent kinetics and prevalence of kiss-and-run and reuse at hippocampal synapses studied with novel quenching methods. *Neuron*. 49:243–256.
- Richards, D. A., J. Bai, and E. R. Chapman. 2005. Two modes of exocytosis at hippocampal synapses revealed by rate of FM1–43 efflux from individual vesicles. *J. Cell Biol.* 168:929–939.
- Fulop, T., S. Radabaugh, and C. Smith. 2005. Activity-dependent differential transmitter release in mouse adrenal chromaffin cells. *J. Neurosci.* 25:7324–7332.
- Aravanis, A. M., J. L. Pyle, and R. W. Tsien. 2003. Single synaptic vesicles fusing transiently and successively without loss of identity. *Nature*. 423:643–647.
- Han, X., C. T. Wang, J. Bai, E. R. Chapman, and M. B. Jackson. 2004. Transmembrane segments of syntaxin line the fusion pore of Ca2+-triggered exocytosis. *Science*. 304:289–292.
- Mayer, A. 2001. What drives membrane fusion in eukaryotes? *Trends Biochem. Sci.* 26:717–723.
- Monck, J. R., and J. M. Fernandez. 1994. The exocytotic fusion pore and neurotransmitter release. *Neuron*. 12:707–716.
- Lindau, M., and W. Almers. 1995. Structure and function of fusion pores in exocytosis and ectoplasmic membrane fusion. *Curr. Opin. Cell Biol.* 7:509–517.
- Kroch, A. E., and K. G. Fleming. 2006. Alternate interfaces may mediate homomeric and heteromeric assembly in the transmembrane domains of SNARE proteins. *J. Mol. Biol.* 357:184–194.
- Hofmann, M. W., K. Peplowska, J. Rohde, B. C. Poschner, C. Ungermann, and D. Langosch. 2006. Self-interaction of a SNARE transmembrane domain promotes the hemifusion-to-fusion transition. *J. Mol. Biol.* 364:1048–1060.
- Roy, R., R. Laage, and D. Langosch. 2004. Synaptobrevin transmembrane domain dimerization-revisited. *Biochemistry*. 43:4964–4970.
- Jackson, M. B. 2007. In search of the fusion pore of exocytosis. *Biophys. Chem.* 126:201–208.
- Jena, B. P. 2003. Fusion pore or porosome: structure and dynamics. *J. Endocrinol.* 176:169–174.
- Cho, S. J., M. Kelly, K. T. Rognlien, J. A. Cho, J. K. Horber, and B. P. Jena. 2002. SNAREs in opposing bilayers interact in a circular array to form conducting pores. *Biophys. J.* 83:2522–2527.
- Bhalla, A., M. C. Chicka, W. C. Tucker, and E. R. Chapman. 2006. Ca(2+)-synaptotagmin directly regulates t-SNARE function during reconstituted membrane fusion. *Nat. Struct. Mol. Biol.* 13:323–330.
- Lin, R. C., and R. H. Scheller. 1997. Structural organization of the synaptic exocytosis core complex. *Neuron*. 19:1087–1094.

32. Bowen, M. E., K. Wenginger, A. T. Brunger, and S. Chu. 2004. Single molecule observation of liposome-bilayer fusion thermally induced by soluble N-ethyl maleimide sensitive-factor attachment protein receptors (SNAREs). *Biophys. J.* 87:3569–3584.
33. Liu, T., W. C. Tucker, A. Bhalla, E. R. Chapman, and J. C. Weisshaar. 2005. SNARE-driven, 25-millisecond vesicle fusion in vitro. *Biophys. J.* 89:2458–2472.
34. Abdulreda, M. H., and V. T. Moy. 2007. Atomic force microscope studies of the fusion of floating lipid bilayers. *Biophys. J.* 92:4369–4378.
35. Chen, A., and V. T. Moy. 2002. Single-molecule force measurements. *Methods Cell Biol.* 68:301–309.
36. Hutter, J. L., and J. Bechhoefer. 1993. Calibration of atomic-force microscope tips. *Rev. Sci. Instrum.* 64:1868–1873.
37. Bennett, M. K., N. Calakos, and R. H. Scheller. 1992. Syntaxin: a synaptic protein implicated in docking of synaptic vesicles at pre-synaptic active zones. *Science.* 257:255–259.
38. Tucker, W. C., T. Weber, and E. R. Chapman. 2004. Reconstitution of Ca(2+)-regulated membrane fusion by synaptotagmin and SNAREs. *Science.* 304:435–438.
39. Liu, W., V. Montana, J. Bai, E. R. Chapman, U. Mohideen, and V. Pappas. 2006. Single molecule mechanical probing of the SNARE protein interactions. *Biophys. J.* 91:744–758.
40. Yersin, A., H. Hirling, P. Steiner, S. Magnin, R. Regazzi, B. Huni, P. Huguenot, P. De los Rios, G. Dietler, S. Catsicas, and S. Kasas. 2003. Interactions between synaptic vesicle fusion proteins explored by atomic force microscopy. *Proc. Natl. Acad. Sci. USA.* 100:8736–8741.
41. Schuette, C. G., K. Hatsuzawa, M. Margittai, A. Stein, D. Riedel, P. Kuster, M. Konig, C. Seidel, and R. Jahn. 2004. Determinants of liposome fusion mediated by synaptic SNARE proteins. *Proc. Natl. Acad. Sci. USA.* 101:2858–2863.
42. McNew, J. A., T. Weber, D. M. Engelman, T. H. Sollner, and J. E. Rothman. 1999. The length of the flexible SNAREpin juxtamembrane region is a critical determinant of SNARE-dependent fusion. *Mol. Cell.* 4:415–421.
43. McNew, J. A., T. Weber, F. Parlati, R. J. Johnston, T. J. Melia, T. H. Sollner, and J. E. Rothman. 2000. Close is not enough: SNARE-dependent membrane fusion requires an active mechanism that transduces force to membrane anchors. *J. Cell Biol.* 150:105–117.